



Non-glycosylated BMP-2 can induce ectopic bone formation at lower concentrations compared to glycosylated BMP-2

F.C.J. van de Watering^a, J.J.J.P. van den Beucken^a, S.P. van der Woning^b, A. Briest^c, A. Eek^d, H. Qureshi^e, L. Winnubst^e, O.C. Boerman^d, J.A. Jansen^{a,*}

^a Department of Biomaterials, Radboud University Nijmegen Medical Center, PO Box 9101, 6500 HB Nijmegen, The Netherlands

^b Department of Cell and Applied Biology, Radboud University Nijmegen, PO Box 9010, 6500 GL Nijmegen, The Netherlands

^c OSSACUR AG, Benzstrasse, D-71720, Oberstenfeld, Germany

^d Department of Nuclear Medicine, Radboud University Nijmegen Medical Center, PO Box 9101, 6500 HB, Nijmegen, The Netherlands

^e Inorganic Membranes, MESA + Institute for Nanotechnology, University of Twente, P.O. Box 217, 7500 AE Enschede, The Netherlands

ARTICLE INFO

Article history:

Received 21 August 2011

Accepted 29 December 2011

Available online 5 January 2012

Keywords:

Bone substitute material

Growth factor release

rhBMP-2

In vivo response

ABSTRACT

Bone morphogenic protein-2 (BMP-2) is a well-known growth factor that can improve the biological performance of bone substitute materials. BMP-2 produced via bacterial expression systems are non-glycosylated (ng) whereas native and recombinant equivalents produced in mammalian cell expression systems are glycosylated (g) proteins. ngBMP-2 is less soluble, resulting in lower BMP-2 release from carriers as used as bone substitute materials. This seems promising for reducing the amount of included growth factor in bone substitute materials. Hence, it was hypothesized that ngBMP-2 would induce formation of the same amount of bone at an ectopic site at lower dosage as gBMP-2. To that end, gBMP-2 and ngBMP-2 were firstly in vitro comparatively evaluated for biological activity and release from a calcium phosphate (CaP) based bone substitute material. Thereafter, an ectopic implantation model in rats was used, in which gBMP-2 and ngBMP-2 were loaded in various dosages (2–20 µg/implant) on the CaP-based bone substitute material and implanted for 4 and 12 weeks. The results revealed that both the in vitro biological activity of and the in vitro release of ngBMP-2 are lower compared to gBMP-2. Upon ectopic implantation, however, ngBMP-2 loaded implants induced more bone formation at lower concentrations from 4-weeks onward compared to gBMP-2 equivalents, indicating the value of ngBMP-2 as a potential alternative for mammalian produced recombinant BMP-2 for bone regenerative therapies.

© 2012 Elsevier B.V. All rights reserved.

1. Introduction

Bone tissue is one of the most frequently transplanted tissues in many fields, including dentistry and orthopedics [1]. Autologous bone grafts are still considered as the golden standard, albeit that several major drawbacks are related to the transplantation of autologous bone, such as postoperative morbidity, low availability and lack of functional shape of the transplantable tissue. Consequently, research is focusing on the development and evaluation of (synthetic) materials to replace autologous bone in grafting procedures.

Alternative (synthetic) materials for bone grafting are predominantly explored within calcium-based ceramics or cements [2,3], bioactive glasses [4], polymer-based materials [5], and combinations thereof [6,7]. Preferably, such synthetic bone substitute materials

have osteogenic, osteoinductive, and osteoconductive properties meaning that similar to autologous bone grafts, bone substitute materials are capable of forming new bone tissue, inducing cells to differentiate into osteoblasts, acting as a three-dimensional structure onto which new tissue can grow, respectively. However, many bone substitute materials do not possess all of these characteristics. This makes that such materials are suitable for use in small, well-vascularized areas, but not for bone regenerative treatments in large, critical-sized defects or under compromised medical conditions. Consequently, strategies to enrich (synthetic) materials with biological factors (e.g. cytokines, chemokines, and growth factors) are necessary in order to improve their biological performance.

Several members of the transforming growth factor- β family are renowned for their capacity to induce bone formation [8–10], of which the so-called bone morphogenetic proteins (BMPs) are frequently used in bone tissue engineering [8,11]. BMPs, more specifically BMP-2, play a significant role in the regulation of many steps in bone morphogenesis due to their biological functions that include chemotaxis, differentiation, and mitosis of bone forming cells [11]. For the delivery of BMP-2 to a defect site, suitable carriers are

* Corresponding author at: Dept. of Biomaterials (309), Radboud University Nijmegen Medical Center, PO Box 9101, 6500 HB Nijmegen, The Netherlands. Tel.: +31 24 3614006; fax: +31 24 3614657.

E-mail address: J.Jansen@dent.umcn.nl (J.A. Jansen).

URL: <http://www.biomaterials-umcn.nl> (J.A. Jansen).

necessary to provide effective availability of BMP-2 to induce differentiation of bone regenerative cells and contribute to bone defect healing [12]. It has been reported that addition of BMP-2 to natural and synthetic polymers [13–15], hydrogels [16], ceramics [17,18] or composites materials [19,20] as a carrier results in sustained release and bone formation. It is assumed that the scaffold material needs to be loaded with an “above threshold” amount of exogenous BMP to actuate bone regenerative cells to contribute to bone formation [12,21,22]. However, the absolute BMP-2 amounts required to stimulate bone formation vary among the different scaffold materials, emphasizing the lack of consensus on suitable loading amounts [12]. For example, the BMP-2 amounts used in calcium phosphate cement-based materials range from 2 [20] to 30 μg [23]. Either from a biological point of view as well as cost effectiveness, research is focusing on the reduction of the included growth factor.

Native BMPs and recombinant equivalents produced in mammalian cells are post-translationally modified through N-linked glycosylation [24], which is a major factor affecting the solubility of BMP-2. Bacterially produced BMPs lack this glycosylation, leading to a decrease in solubility. Hence, the use of the less soluble non-glycosylated BMP-2 might allow the application of lower BMP doses to induce bone formation [25].

In the present study, the bioactivity and osteoinductive properties of non-glycosylated BMP-2 (ngBMP-2) and glycosylated BMP-2 (gBMP-2) were comparatively evaluated. In vitro bioactivity assays, an in vitro release assay and an in vivo rat subcutaneous model using pre-set calcium phosphate cement (CPC) with adsorbed BMP-2, were used to assess the in vitro bioactivity, in vitro release profile and to evaluate the ectopic osteoinductive potential of a carrier loaded with ngBMP-2 compared to gBMP-2. It was hypothesized that ngBMP-2 was biologically active and capable of inducing differentiation and mineralization of osteoblast-like cells. In addition, it was hypothesized that due to the effects of glycosylation on solubility the retention of ngBMP-2 to CPC would be higher, resulting in the induction of bone at an ectopic site at lower concentrations compared to gBMP-2 loaded equivalents.

2. Materials and methods

2.1. Materials

Calcium phosphate cement (CPC) consisted of 85% alpha tricalcium phosphate (α -TCP; CAM Bioceramics BV, Leiden, The Netherlands), 10% dicalcium phosphate anhydrous (DCPA; J.T. Baker Chemical Co., USA) and 5% precipitated hydroxyapatite (pHA; Merck, Darmstadt, Germany). The CPC powders were ball-milled and had particle sizes of $9.7 \pm 2.0 \mu\text{m}$, $4.5 \pm 1.9 \mu\text{m}$, and $5.0 \pm 1.9 \mu\text{m}$ for α -TCP, pHA, and DCPA, respectively [26]. The cement liquid applied was a sterilized 2 wt.% aqueous solution of Na_2HPO_4 . Acid terminated poly(DL-lactic-co-glycolic acid) (PLGA; Purasorb®, Purac, Gorinchem, the Netherlands) with a lactic to glycolic acid ratio of 50:50 and a molecular weight (M_w) of $17 \pm 0.02 \text{ kg/mol}$ was used for microparticle preparation. Recombinant human ngBMP-2 was kindly provided by Dr. P. Hortschansky (Hans Knoell Institute, Jena, Germany). Commercially available recombinant human glycosylated BMP-2 (gBMP-2; R&D Systems MN, USA) was used for comparison.

2.2. In vitro studies

2.2.1. Bioactivity assay with C2C12 cell line

The biological activity of both gBMP-2 and ngBMP-2 was tested by the induction of alkaline phosphatase (ALP) activity in C2C12 cells, as described before [27]. C2C12 cells were plated at a density of $2 \times 10^4 \text{ cells/cm}^2$ and grown for 24 h in Dulbecco's Modified Eagle Medium (DMEM; Gibco BRL Life Technologies B.V., Breda, The Netherlands) supplemented with 10% fetal calf serum (FCS; Gibco).

Subsequently, medium was replaced by DMEM containing 5% FCS either in the presence or absence of 1–1000 ng/ml ngBMP-2 or gBMP-2. After 72 h ALP enzymatic activity was quantified by measuring the formation of p-nitrophenol from p-nitrophenyl phosphate (PNPP, Sigma-Aldrich, St. Louis, MO, USA) as described previously [28]. ALP enzymatic activity was corrected for differences in cell number as determined by a Neutral Red assay [29].

2.2.2. Bioactivity assay with primary rat bone marrow-derived osteoblast-like cells

Two independent runs were performed, with for each run freshly isolated primary rat bone marrow-derived osteoblast-like cells (OBLCs) following the procedure described by Maniopoulos et al. [30]. All procedures were conducted in accordance with ISO-standards (9001:2008) and National Guidelines for care and use of laboratory animals after approval of the Experimental Animal Ethical Committee (RU-DEC 2008–199). In short, bone marrow was harvested from femora of male Wistar rats weighing between 120 g and 150 g. Femora were washed 3 times in α -minimal essential medium (α -MEM; Gibco) containing 0.5 mg/ml gentamycin (Gibco) and 3.0 $\mu\text{g/ml}$ Fungizone (Gibco). Epiphyses were cut off and diaphyses flushed out with 9 ml non-osteogenic medium (i.e. α -MEM supplemented with 10% FCS (Gibco) and 50 mg/ml gentamycin (Gibco)). The cells were divided into 2 groups; one group cultured in non-osteogenic medium and the other group in osteogenic medium (i.e. α -MEM supplemented with 10% FCS (Gibco), 50 $\mu\text{g/ml}$ ascorbic acid (Sigma), 10 mM Na β -glycerophosphate (Sigma), 10^{-8} M dexamethasone (Sigma) and 50 $\mu\text{g/ml}$ gentamycin (Gibco)). The cells were incubated in culture flasks at 37 °C in a humidified atmosphere of 95% normal air and 5% carbon dioxide. The medium was changed 3 times per week. After 7 days of primary culture, the cells were detached using trypsin/ethylenediaminetetraacetic acid (EDTA) (0.25% w/v trypsin/0.02% EDTA), concentrated via centrifugation, resuspended in either non- or osteogenic medium, and seeded at a concentration of $1 \times 10^4 \text{ cells/cm}^2$ in 24-well plates (medium volume: 1 ml). Cell culture was maintained using 4 different conditions: (1) non-osteogenic medium (–O); (2) ngBMP-2-supplemented non-osteogenic medium (500 ng/ml) (–OBMP); (3) osteogenic medium (+O); and (4) ngBMP-2 supplemented osteogenic medium (500 ng/ml) (+OBMP). The medium was changed 3 times a week. For respective groups, ngBMP-2 was added during the first week at medium refreshments at days 0, 1, 3 and 5. *Protein assay*: To determine cell amounts, total protein measurements were performed using the bicinchoninic acid (BCA) assay (Sigma) on day 4, 8, 12 and 16 ($n=3$). The culture medium was removed and the cells were washed twice with PBS. After washing, 1 ml of MilliQ was added to each sample and the samples were stored at $-80 \text{ }^\circ\text{C}$. Just before analysis, the samples were subjected to two freeze-thaw cycles. A standard curve was made using serial dilutions of bovine serum albumin in MilliQ (range: 0–40 $\mu\text{g/ml}$). Then, 100 μl of sample or standard was added to the wells of a 96-wells plate and 100 μl of work solution (1% copper sulfate, 25% BCA in MilliQ and 24% sodium carbonate, sodium bicarbonate, sodium tartrate in 0.2 N NaOH) was added to all the wells. The samples were incubated at 37 °C for 2 h and left to cool down at room temperature. The 96-wells plate was read (Bio-Tek Instruments, Abcoude, the Netherlands) at 570 nm, and the protein concentrations were calculated from the obtained standard curve. *Alkaline Phosphatase Activity (ALP) assay*: ALP was used as a marker for early osteoblast differentiation. For determination of ALP-activity, the same samples as for the protein assay were used. ALP-activity was determined by adding 80 μl of the samples and 20 μl of buffer solution (5 mM magnesium chloride, 0.5 M 2-amino-2methyl-1-propanol) to a 96-wells plate. A standard curve was prepared via serial dilutions of 4-nitrophenol (range: 0–25 nM), after which 100 μl was added to a 96-wells plate. 100 μl of substrate solution (5 mM p-nitrophenylphosphate) was added to all wells and

the plate was incubated for 1 h at 37 °C. The reaction was stopped by adding 100 μ l of stop solution (0.3 M sodium hydroxide) to all the wells. The plate was read at 405 nm, and ALP-activity values were normalized to the amount of cellular protein present in the samples. **Calcium assay:** To assess the formation of mineralized matrix, culture plates were washed with PBS and 1 ml of 0.5 N acetic acid was added to the samples for overnight incubation during gentle agitation. A standard curve was made using serial dilutions of $\text{CaCl}_2 \cdot 2\text{H}_2\text{O}$ in acetic acid (range: 0–100 μ g/ml). Then, 10 μ l of the sample or standard was added to the wells of a 96-wells plate and 300 μ l of work solution (5% o-cresolphthalein complexone, 5% 14.8 M ethanolamine, 2% hydroxyquinoline and 88% MilliQ) was added to all wells. Samples were incubated for 5 to 10 min at room temperature after which the plate was read at 570 nm.

2.3. Release experiment and in vivo studies

2.3.1. Preparation of PLGA-microparticles, pre-set CPC scaffolds and loading with BMP-2

PLGA-microparticles (~40 μ m diameter) were prepared using a double-emulsion-solvent-extraction technique (water-in-oil-in-water), as described previously [31]. In brief, microparticles were produced by adding 500 μ l of distilled water to 1400 mg PLGA in 2 ml dichloromethane. The mixture was emulsified using a Turrax® emulsifier for 60 s at 6000 rpm. Then, 6 ml 0.3% aqueous poly (vinyl alcohol) (PVA, Acros Organics, Geel, Belgium) solution was added and emulsified for another 60 s at 6000 rpm to produce a second emulsion. The emulsion was transferred to a stirred beaker, after which 394 ml 0.3% PVA solution and 400 ml of 2% isopropyl alcohol solution was added slowly. After 1 h of stirring, the microparticles were allowed to sediment for 15 min and the solution was decanted. Then, the microparticles were washed and collected through centrifugation at 1500 rpm for 5 min, lyophilized and stored at –20 °C until use. Pre-set CPC scaffolds were prepared by adding 300 mg PLGA-microparticles to 700 mg CPC powder into a closed tip 2 mL plastic syringe (BD Plastipak™, Becton Dickinson S.A., Madrid, Spain), after which the content was stirred vigorously for 20 s to achieve homogenous distribution of microparticles within the cement powder (Silamat® mixing apparatus, Vivadent, Schaan, Liechtenstein). Subsequently, 2 wt.% Na_2HPO_4 was added to the mixture in a liquid/powder ratio of 0.35 and mixed for 20 s using a mixing apparatus. After mixing, the cement was immediately injected in a Teflon mold to ensure a standardized shape of the scaffolds (\varnothing 7.8 mm, height 2.8 mm) and placed overnight at 37 °C. To create an instantaneous open porous structure, the pre-set scaffolds were placed in a furnace at 650 °C for 2 h to burn out the polymer. Finally, CPC scaffolds were sterilized by autoclaving and characterized using scanning electron microscopy (SEM; JEOL6310 at 15 kV). The total porosity of the samples was calculated by the following equation [31]:

$$\varepsilon_{\text{tot}} = \left(1 - \frac{m_{\text{burnt}}}{V \cdot \rho_{\text{HAP}}}\right) * 100\%$$

ε_{tot} = total porosity (%)
 m_{burnt} = average mass sample (after burning out polymer) (g)
 V = volume sample (cm^3)
 ρ_{HAP} = density hydroxyl apatite (g/cm^3)

To measure the open interconnective porosity of the burned-out pre-set CPC scaffolds, mercury (Hg) porosimetry was performed using PoreMaster® GT mercury intrusion porosimeter (Quantachrome instruments, Odelzhausen, Germany). Burned-out pre-set CPC scaffolds were placed into the system and the intrusion of Hg was analyzed under low pressure conditions. Loading of the burned-out pre-set CPC scaffolds

with BMP-2 was performed via adsorption. Therefore, a volume of 30 μ l growth factor solution containing 1, 5 or 10 μ g gBMP-2 or ngBMP-2 was applied to the surface of each side of the scaffold to obtain final amounts of 2, 10 or 20 μ g BMP-2/scaffold. Thereafter, the scaffolds were frozen and lyophilized. To visualize the distribution of the added drugs within the burned-out pre-set CPC scaffolds, albumin from bovine serum (BSA) labeled with alexa fluor 488 (Invitrogen, Life Technologies Europe BV, Bleiswijk, The Netherlands) was used as model protein. The loading of labeled BSA (2, 10 or 20 μ g BSA/scaffold) to the CPC was similar as described previously. Thereafter, the scaffolds were frozen and lyophilized. The BSA loaded CPC were overnight fixed in 4% formalin. Subsequently, the tissue blocks were embedded in methylmethacrylate. Perpendicularly through the implants, thin sections (10 μ m) were prepared using a microtome with diamond blade (Leica Microsystems SP 1600, Nussloch, Germany) [32]. The sections were visualized using a reflectant fluorescence microscope with a Zeiss filter set 00, consisting of a 530–585 nm band-pass excitation filter (Carl Zeiss B.V., Sliedrecht, The Netherlands).

2.3.2. Release experiment

gBMP-2 and ngBMP-2 were labeled with ^{125}I , as described previously [33]. Briefly, in a 500 μ l eppendorf tube coated with 100 μ g iodogen, 10 μ l of 0.5 M phosphate buffer saline (PBS) was added. Growth factor (25 μ g) and 10–15 MBq ^{125}I (Perkin-Elmer, Boston, MA) was added and incubated at room temperature for 10 min, after which 100 μ l of saturated tyrosine solution in PBS was added. The labeling efficiency of the reaction was 67.6% and 23% for gBMP-2 and ngBMP-2, respectively. To remove the non-bound ^{125}I , the reaction mixture was eluted using 0.1% BSA in PBS on a pre-rinsed disposable Sephadex G25M column (PD-10; Pharmacia, Uppsala, Sweden). The specific activity of the labeled protein was 18.7 $\mu\text{Ci}/\mu\text{g}$ for gBMP-2 and 9.1 $\mu\text{Ci}/\mu\text{g}$ for ngBMP-2. CPC scaffolds were loaded similarly as described above with either ^{125}I -gBMP-2 or ^{125}I -ngBMP-2 solutions using a hot/cold mixture of BMP-2, containing 1 μCi per scaffold (for gBMP 1 μCi ~0.053 μg BMP-2; for ngBMP 1 μCi ~0.110 μg BMP-2). A volume of 30 μ l ^{125}I -gBMP-2 or ^{125}I -ngBMP-2 hot/cold solution containing 1, 5 or 10 μ g BMP-2 was carefully loaded onto the surface of each side of the scaffold to obtain final amounts of 2, 10 or 20 μ g BMP-2/scaffold. Thereafter, the scaffolds were frozen and lyophilized. CPC scaffolds loaded with ^{125}I -labeled BMP-2 ($n=3$) were placed in 10 ml glass vials for evaluation of in vitro BMP-2 release kinetics and incubated in 3 ml PBS at 37 °C on an orbital shaker at low rotational speed (60 rpm) for 28 days. At days 1, 4, 7, 14, 21 and 28, the samples were carefully transferred to new vials containing fresh PBS, after which gamma emission of the samples was measured in a shield well-type gamma counter (Wizard, Pharmacia-LKB, Uppsala, Sweden). Standards were measured simultaneously to correct for radioactive decay. The remaining activity in the scaffolds was expressed as percentage of the initial dose.

2.3.3. Surgical procedure

Twenty-four healthy young adult (8 weeks old) male Wistar rats were used as experimental animals. National guidelines for the care and use of laboratory animals were observed. The research was reviewed and approved by the Experimental Animal Committee of the Radboud University (RUDEC 2010–062). Anesthesia was induced and maintained by isoflurane inhalation (Rhodia Organique Fine Limited, Avonmouth, Bristol, UK). To minimize post-operative discomfort, Rimadyl (Carprofen, Pfizer Animal Health, New York, USA) was administered intraperitoneally (5 mg/kg) before the surgery, directly after the surgery and subcutaneously for two days after surgery. Four CPC scaffolds were subcutaneously implanted into the back of each rat. To insert the scaffolds, rats were immobilized on their abdomen and the skin was shaved and disinfected with chlorhexidine. On both sides of the vertebral column, two small paravertebral incisions were made through the full thickness of the skin. Lateral to the

incisions, a subcutaneous pocket was created using blunt dissection. Subsequently, one implant was inserted into each pocket. Finally, the skin was closed using staples (Agraven, Instruvet, Boxmeer, The Netherlands). In total, ninety-six implants were placed according to a randomization scheme ($n = 8$ for each group per implantation period). The animals were housed in pairs. In the initial postoperative period, the intake of water and food was monitored. Further, the animals were observed for signs of pain, infection and proper activity. At the end of the implantation time, the rats were sacrificed by CO_2 -suffocation.

2.3.4. Implant retrieval and histological preparations

Implants were retrieved after a 4 or 12 week implantation period. After sacrifice, implants with surrounding tissue were excised and fixed in 4% formalin. Subsequently, the tissue blocks were dehydrated in increasing ethanol concentrations (70–100%) and embedded in methylmethacrylate. Perpendicularly through the implants, thin sections ($10 \mu\text{m}$) were prepared using a microtome with diamond blade (Leica Microsystems SP 1600, Nussloch, Germany) [32]. Three sections of each implant were stained with methylene blue and basic fuchsin and examined using light microscopy (Leica Microsystems AG, Wetzlar, Germany). From the control, 20 $\mu\text{g}/\text{cement}$ ngBMP-2 and gBMP-2 12 weeks implantation groups, MMA samples were polished and gold sputter-coated prior to analysis with Scanning electron microscopy (JEOL 6330) using Back-Scattered Electron (BSE) mode for histomorphometrical analysis. Using BSE mode, it is possible to distinguish bone from the implanted scaffold based on the respective densities of the two substances. In addition, two samples of the 20 $\mu\text{g}/\text{cement}$ ngBMP-2 and gBMP-2 12 weeks implantation group were deplastified, decalcified (Sakura Finetek, Syntec Scientific, Dublin, Ireland) for 16 h, dehydrated through a series of graded ethanol and embedded in paraffin. Using a microtome (Leica RM 2165, Leica Microsystems, Nussloch, Germany), $6 \mu\text{m}$ thick sections were prepared and stained with Goldner Trichrome.

2.3.5. Histological and histomorphometrical evaluation

Sections of MMA-embedded specimens (at least 3 sections per specimen) were quantitatively assessed using computer-based image analysis techniques (Leica® Qwin Pro-image analysis system, Wetzlar, Germany). From digital images (magnification: $5\times$), the total amount of newly-formed bone surrounding the CPC scaffold was determined and expressed in area measures (mm^2). Sections of decalcified, paraffin-embedded specimens stained with Haematoxyline–eosine and Goldner trichrome (at least 3 sections per specimen) were qualitatively examined for tissue ingrowth.

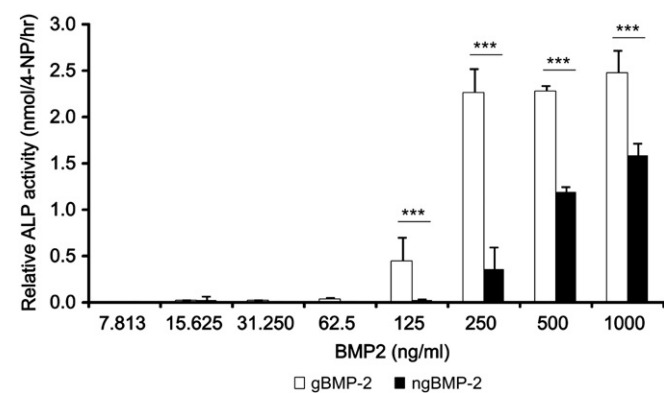


Fig. 1. ALP activity of the C2C12 cells after 72 h stimulation with gBMP-2 or ngBMP-2. C2C12 cells demonstrate a dose-dependent ALP-activity. ALP-activity was significantly increased by gBMP-2, and ngBMP-2. Results are shown as means \pm SD of triplicate samples for one representative experiment out of two. (***) $p < 0.001$.

2.4. Statistical analyses

Statistical analysis of the in vitro bioactivity assay measurements was performed using GraphPad Instat 3.05 software (GraphPad Software Inc., San Diego, CA) using one-way analysis of variance with a Tukey multiple comparison post test. Differences were considered significant at p -values less than 0.05. Statistical analysis of the release experiment measurements was performed using SPSS, version 16.0

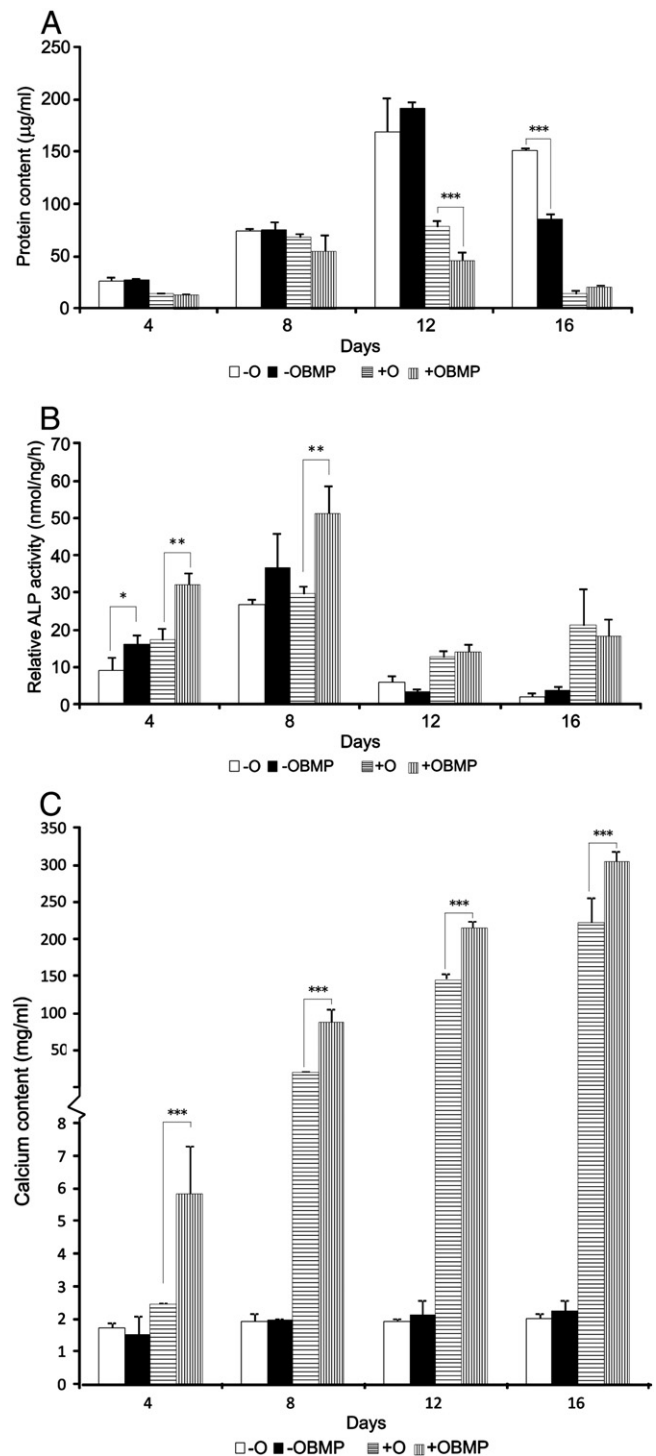


Fig. 2. (A) Cellular protein content and (B) Alkaline phosphatase (ALP) activity of and (C) mineralization (calcium deposition) by rat osteoblast-like cells cultured in non-osteogenic (–O) or osteogenic (+O) medium in the presence or absence of ngBMP-2. Results are shown as mean \pm SD of triplicate samples for one representative experiment out of two. (***) $p < 0.001$.

(SPSS INC., Chicago, Illinois USA). The statistical comparisons were performed using 2-tailed Student's *t*-test. Differences were considered significant at *p*-values less than 0.05. Statistical analysis of bone formation measurements was performed using SPSS, version 16.0 (SPSS INC., Chicago, Illinois USA). The statistical comparisons were performed using a one-way analysis of variance (ANOVA) with a Tukey multiple comparison post-test. Differences were considered significant at *p*-values less than 0.05.

3. Results

3.1. In vitro studies

Two independent runs of the bioactivity assay with C2C12 cells showed similar results. C2C12 cells cultured in the presence of the different types of BMP-2 demonstrated a dose-dependent ALP-activity. The threshold for the detection of ALP-activity was ~125 ng/ml for gBMP-2 and 250 ng/ml for ngBMP-2 with significant higher values ($p < 0.001$) for gBMP-2 at each concentration (Fig. 1). Two independent runs of cell culture experiments with primary rat bone marrow derived OBLCs showed similar results. OBLCs cultured in all types of medium showed an increase in the cellular protein content between day 4 and 12 after cell seeding, with higher maximum values for –O and –OBMP. Thereafter, the protein content in all experimental groups decreased (Fig. 2a). For all experimental groups, ALP-activity was observed from day 4 onwards, showing maximum values at day 8 (Fig. 2b). In general, ngBMP-2 addition significantly increased ALP-activity in –O as well as +O in the first 8 days of culture. For mineralization (Fig. 2c), a gradual increase in calcium amounts was observed from day 4 onward for +O and +OBMP. Significantly higher values ($p < 0.001$) were observed for +OBMP compared to +O at each individual time point. For –O and –OBMP, no increase in calcium amounts was observed.

3.2. CPC scaffolds, drug loading and release experiment

CPC scaffolds were characterized using SEM (Fig. 3) and demonstrated different types of porosity: intrinsic microporosity (pore size ~10 nm–100 nm) related to material setting and crystallization, and macroporosity (pore size: ~40 μ m) resulting after burning out

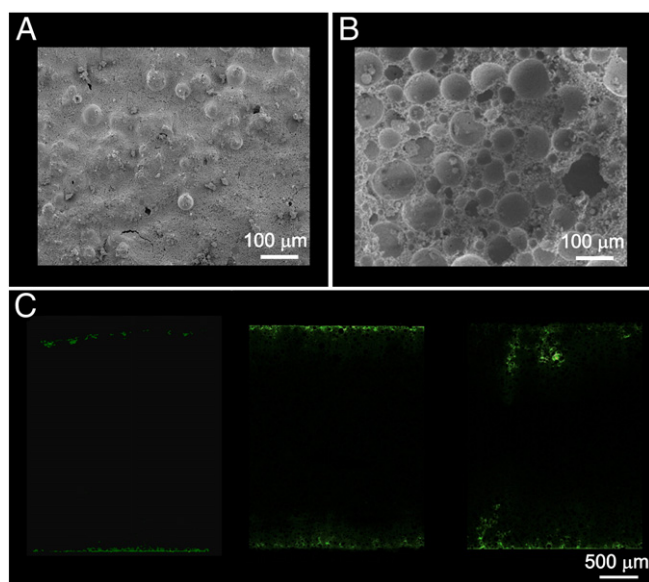


Fig. 3. Characterization of porous CPC scaffolds. Microscopic SEM micrographs of composite material before (A) and after (B) burning out the PLGA-microparticles. Bar represents 100 μ m. (C) The distribution of low, middle or high dose of the model protein alexa fluor 488 labeled BSA within porous CPC scaffolds. Bar represents 500 μ m.

PLGA-microparticles. The total porosity (consisting of the intrinsic porosity of material and additional porosity after PLGA-microparticle degradation) was determined by measuring the weight of pre-set composite disks (with and without PLGA-microparticles) and comparing it to a fictitious, solid hydroxyapatite disk with the same dimensions. The porosity measurements demonstrated a total porosity of $75.5 \pm 1.3\%$. The interconnective porosity as analyzed by Hg intrusion porosimetry revealed a porosity of 21.3%. Drug loading was visualized using cross-sections of CPC-scaffolds loaded with different amounts of alexa fluor 488 labeled BSA (Fig. 3). In all concentrations, the distribution of the protein is only observed peripherally and not in the center of the implants. However, a dose-dependent effect is observed whereby with increasing BSA concentrations the protein infiltration is enlarged. The release and retention after 28 days of ^{125}I -gBMP-2 and ^{125}I -ngBMP-2 for the low (2 μ g), middle (10 μ g), and high (20 μ g) dose implants are depicted in Fig. 4 and Table 1. In general, all scaffolds retained their integrity during the entire experiment and showed an initial burst release within 1 day, followed by a sustained release till day 28 (Fig. 4A). For gBMP-2, the burst release (Fig. 4B) was 17.4 ± 7.8 , 14.3 ± 5.8 and $11.7 \pm 1.0\%$ for low, middle and high dose loaded scaffolds, respectively. For ngBMP-2, the burst release was 16.1 ± 2.4 , 22.0 ± 0.7 and $16.0 \pm 3.8\%$ for low, middle and high dose loaded scaffolds, respectively. The overall sustained release (Fig. 4B; % per day) from day 1–28 of ngBMP-2 compared to gBMP-2 was significantly lower ($p < 0.001$, overall sustained release of $0.63 \pm 0.07\%$ and $0.88 \pm 0.17\%$ for ngBMP-2 and gBMP-2, respectively). Separately, the sustained release from day 1 to day 28 was significantly lower for the low ngBMP-2 loaded scaffolds compared to gBMP-2 loaded scaffolds ($p < 0.05$, sustained release of 0.86 ± 0.15 and $0.56 \pm 0.07\%$ /day for gBMP-2 and ngBMP-2, respectively). A similar tendency was observed for the middle and high ngBMP-2 loaded scaffolds compared to the high gBMP-2 loaded scaffolds (for the middle dosage $p = 0.146$, sustained release of 0.90 ± 0.26 and $0.63 \pm 0.03\%$ /day for gBMP-2 and ngBMP-2, respectively; for the high $p = 0.130$, sustained release of 0.87 ± 0.161 and $0.69 \pm 0.03\%$ /day for gBMP-2 and ngBMP-2, respectively). After 28 days, the total release (Fig. 4B) for gBMP-2 was 40.6 ± 4.0 , 38.7 ± 3.4 and $35.1 \pm 4.5\%$ for low, middle and high dose loaded scaffolds, respectively. For ngBMP-2, the total release was 31.4 ± 2.4 , 39.1 ± 0.5 and $34.6 \pm 3.6\%$ for low, middle and high dose loaded scaffolds, respectively. These release results show significantly increased protein retention for ngBMP-2 in the low loaded groups compared to low gBMP-2 ($p < 0.05$), whereas no significant differences were observed for the middle and high loaded groups.

3.2.1. Descriptive light microscopy

All specimens showed a fibrous capsule surrounding the scaffold after both 4 and 12 weeks of implantation, without the presence of inflammatory cells at the interface. Fig. 5 presents an overview of histological sections of the specimens after each implantation period as well as higher magnifications of the newly-formed bone tissue at the interface between CPC scaffold and tissue. Bone formation was observed for all BMP-2 loaded implants after both 4 and 12 weeks of implantation, but was absent for unloaded controls. Bone formation and fibrous tissue were only observed peripherally and not in the center of the implants in any of the sections (Figs. 5 and 6). Bone formation was most pronounced for high dose ngBMP-2 loaded scaffolds after 12 weeks of implantation.

3.2.2. Histomorphometrical evaluation

Quantitative results of ectopic bone formation are shown in Fig. 7. After 4 weeks of implantation, a dose-dependent amount of bone formation was observed for both gBMP and ngBMP, whereas no bone formation was observed for controls. A significant higher amount of newly-formed bone ($p < 0.001$) was found for low dose ngBMP scaffolds compared to gBMP equivalents. The amount of newly-formed

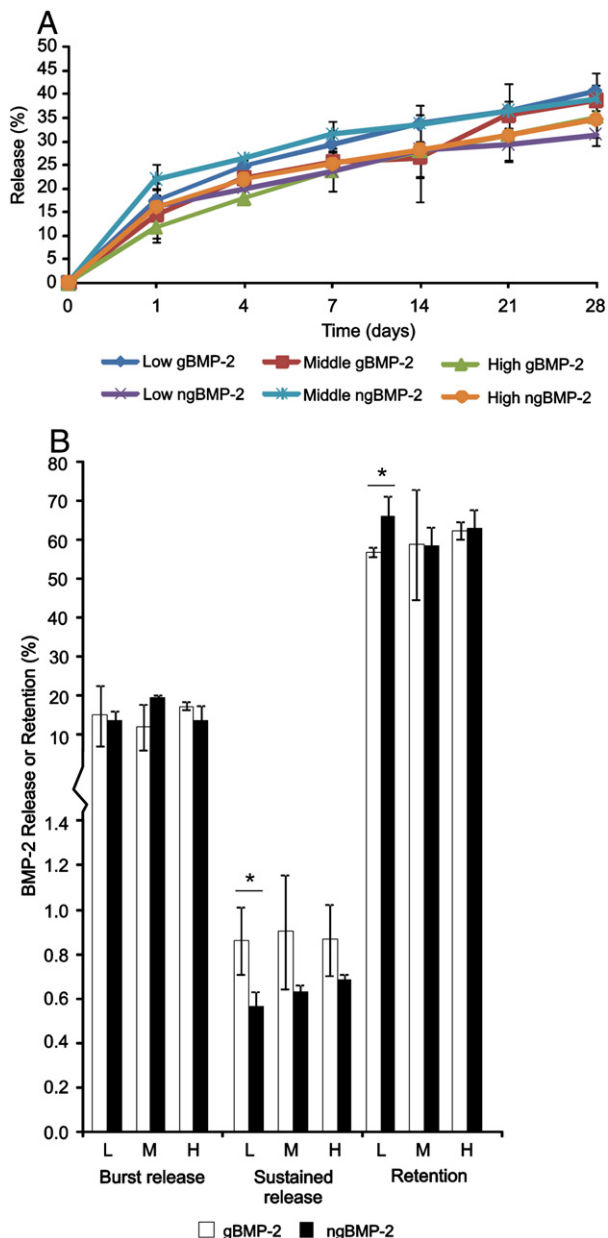


Fig. 4. Longitudinal scintigraphic assessment of low (L), middle (M) and high (H) dose gBMP-2 and ngBMP-2 (A) released from loaded porous CPC scaffolds during 28 days and (B) the in vitro burst release (after 1 day), sustained release (the release per day from day 1–28) and the retention after 28 days. The release and retention is expressed as percentage of the ratio of initial loading amount. Error bars represents the mean \pm SD ($n = 3$). (*) $p < 0.05$.

bone significantly increased in time (for gBMP-2 loaded scaffolds $p < 0.01$; for ngBMP-2 loaded scaffolds $p < 0.001$) for all types of scaffolds (except controls) with a maximum of $\sim 1 \text{ mm}^2$ after 4 weeks to a maximum of $\sim 7 \text{ mm}^2$ after 12 weeks. Similar to week 4 observations, significant higher amounts of newly-formed bone ($p < 0.001$) were found for low dose ngBMP scaffolds compared to gBMP equivalents after 12 weeks of implantation.

4. Discussion

For clinical application, the availability of recombinant human BMP-2 at acceptable costs is mandatory. In view of that, large-scale BMP-2 production via a bacterial host might be a good alternative for mammalian cells for reasons of cost effectiveness [34]. However, bacterially produced BMP-2 lacks a glycosylation site and hence is structurally different to and less soluble than the native, post-translationally modified mammalian BMP-2. Consequently, this study comparatively evaluated the bioactivity of non-glycosylated (ng) and glycosylated (g) BMP-2 using in vitro bioactivity and release assays and an ectopic animal model, in which different amounts (2–20 μg) BMP-2 were loaded onto a porous calcium phosphate cement (CPC) carrier. It was hypothesized that less soluble ngBMP-2 was biologically active and would induce more bone ectopically compared to more soluble gBMP-2. In vitro bioactivity assays revealed that ngBMP-2 is less active than gBMP-2, however ngBMP-2 was still capable of inducing differentiation and mineralization of primary rat osteoblast-like cells. The overall sustained release from day 1–28 of ngBMP-2 was significantly lower as compared with gBMP-2. Separately, a significant decrease in sustained release for low ngBMP-2 loaded scaffolds as compared with gBMP-2 loaded scaffolds was observed leading to an increased amount of retained protein after 28 days. In vivo ectopic bone formation demonstrated that ngBMP-2 is capable of inducing significant more bone at low dosage (2 μg /CPC) from four weeks onward compared to gBMP-2.

The regenerative capacity of BMP-2 is dependent on its ability to stimulate the pre-osteoblastic cells to differentiate into bone forming cells leading to the formation of new bone. In the current study, a difference in levels of the activity of early osteoblastic differentiation marker ALP in C2C12 cells cultured in the presence of ngBMP-2 compared to gBMP-2 was observed. Nevertheless, ngBMP-2 demonstrated to be capable of inducing differentiation and mineralization of primary rat osteoblast-like cells. In contrast, several studies reported equal levels of ALP-activity for cells cultured in the presence of gBMP-2 or ngBMP-2 [35,36] indicating a comparable in vitro potency of both types of BMP-2 as osteoinductive factor. Due to inconsistency in different reports on the efficacy of both types of BMP-2 in in vitro experiments, the precise effect of glycosylation on bioactivity remains unclear.

The release profiles of adsorbed ngBMP-2 and gBMP-2 showed an initial burst release (within 1 day) followed by a sustained release (from day 1–28) of in total approximately $\sim 35\%$ for the ngBMP-2 loaded scaffolds and $\sim 38\%$ for the gBMP-2 loaded scaffolds, which were similar to earlier reported ones, describing a release up to

Table 1
The release in percentage of gBMP-2 and ngBMP-2 from porous CPC.

	Burst release (%)		Cumulative sustained release (%)				
	D 1	D 1	D 4	D 7	D 14	D 21	D 28
Low gBMP-2	17.4 \pm 7.8	17.4 \pm 7.8	24.7 \pm 1.3	29.4 \pm 2.69	33.7 \pm 3.8	36.5 \pm 5.7	40.6 \pm 4.0
Middle gBMP-2	14.3 \pm 5.8	14.3 \pm 5.8	22.2 \pm 1.8	25.7 \pm 2.3	26.5 \pm 9.2	35.5 \pm 3.2	38.7 \pm 3.4
High gBMP-2	11.7 \pm 1.1	11.7 \pm 1.1	17.9 \pm 2.5	23.7 \pm 3.4	27.9 \pm 3.5	31.3 \pm 3.2	35.1 \pm 4.5
Low ngBMP-2	16.1 \pm 2.4	16.1 \pm 2.4	20.1 \pm 3.2	23.6 \pm 4.1	28.2 \pm 5.9	29.3 \pm 3.7	31.4 \pm 2.4*
Middle ngBMP-2	22.0 \pm 0.7	22.0 \pm 0.7	26.4 \pm 0.5	31.5 \pm 2.9*	33.6 \pm 0.3	36.5 \pm 0.8	39.1 \pm 0.5
High ngBMP-2	16.0 \pm 3.8	16.0 \pm 3.8	21.9 \pm 3.5	25.2 \pm 2.5	28.1 \pm 5.4	31.2 \pm 5.1	34.6 \pm 3.6

Low, middle and high: 2 μg , 10 μg or 20 μg loaded carrier with either gBMP-2 or ngBMP-2.

* $p < 0.05$ as compared between both groups at the specific time point.

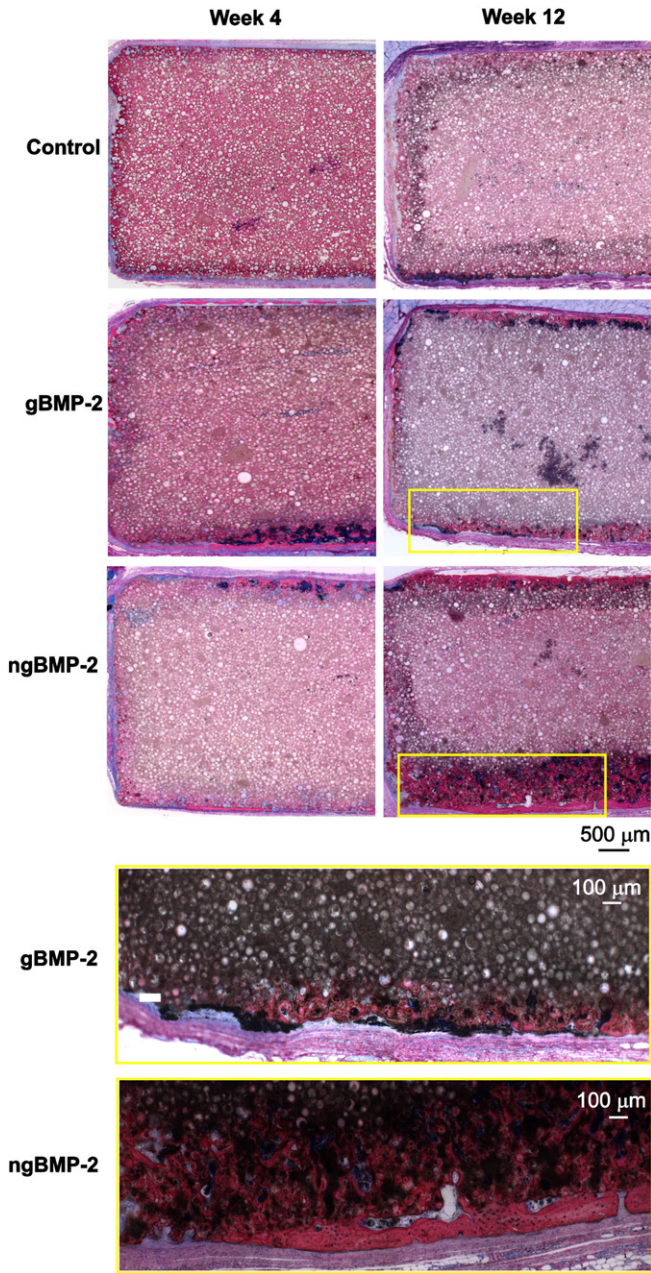


Fig. 5. Histological sections of the low dose gBMP-2 and ngBMP-2 loaded porous CPC scaffolds after 4 and 12 weeks implantation. Bar represents 500 µm. Magnifications of the boxes show low dose gBMP-2 and ngBMP-2 loaded porous CPC scaffolds after 12 weeks of implantation. Bar represents 100 µm. Methylene blue and basic fuchsin staining.

~40% [37]. Despite similar release profiles of both BMPs, the sustained release per day for the low ngBMP-2 loaded scaffolds was significantly reduced and a tendency was observed in the middle and high ngBMP-2 loaded scaffolds compared to gBMP-2 loaded scaffolds. These results are in line with the data of the amounts of BMP-2 retained onto the implants after 28 days, showing significantly higher amounts for low ngBMP-2 compared to low gBMP-2, whereas for middle and high loaded implants similar amounts were observed for ngBMP-2 and gBMP-2. Although after 28 days the BMP-2 retention is only significantly different for the low dosages, the overall sustained release of ngBMP-2 compared to gBMP-2 is significantly lower, indicating an effect of glycosylation on protein release. Interestingly, after a similar implantation period in vivo, low dosages of ngBMP-2 induced significantly more ectopic bone formation compared to low

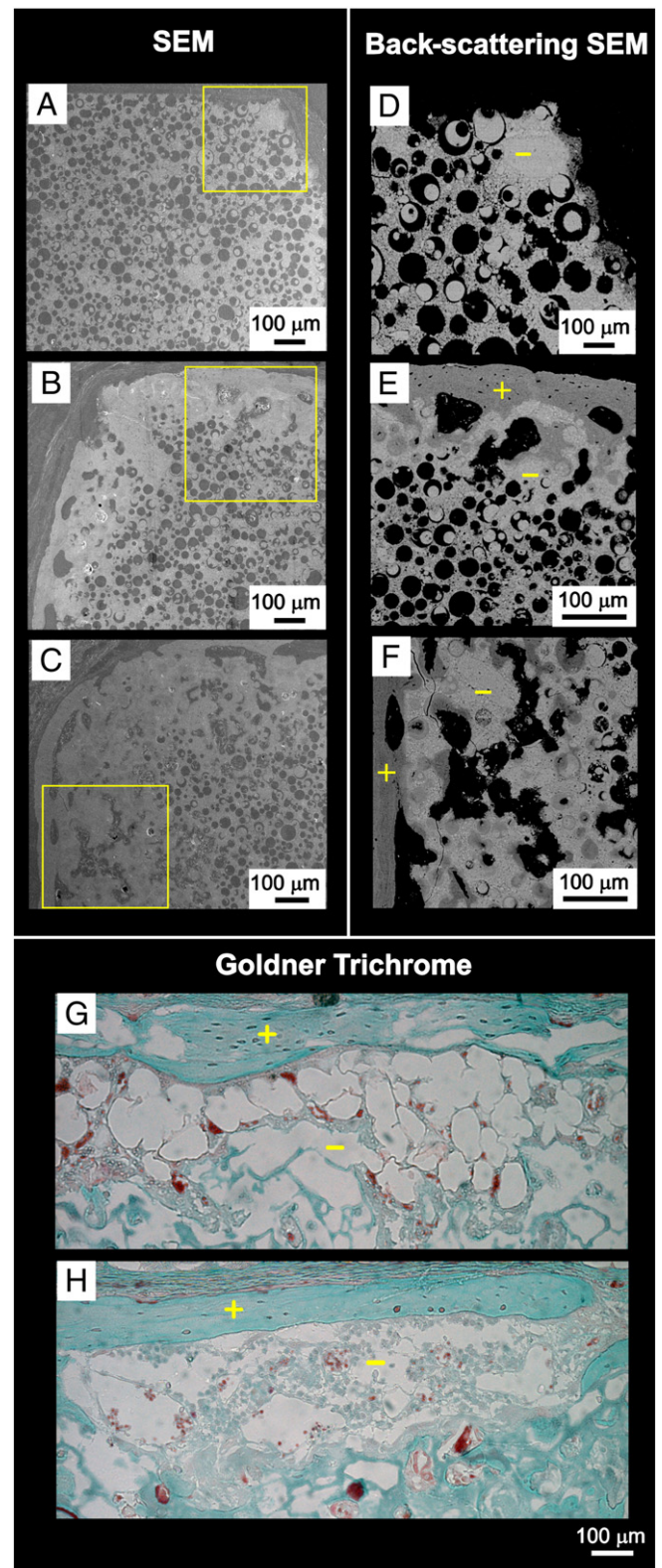


Fig. 6. Cross-sections of Control (A, D) and high dose gBMP-2 (B, E, G) and ngBMP-2 (C, F, H) loaded porous CPC scaffolds after 12 weeks implantation observed with SEM, back scattering SEM and histological with Goldner trichrome staining, respectively. Bone (+) and CPC scaffold (-) are indicated in the back scattering SEM micrographs and Goldner trichrome stained sections.

gBMP-2 dosages. As it is likely that the biological process of bone formation is related to the presence of BMP-2 at the implant and its solubility, the significantly increased amounts of ngBMP-2 retained onto

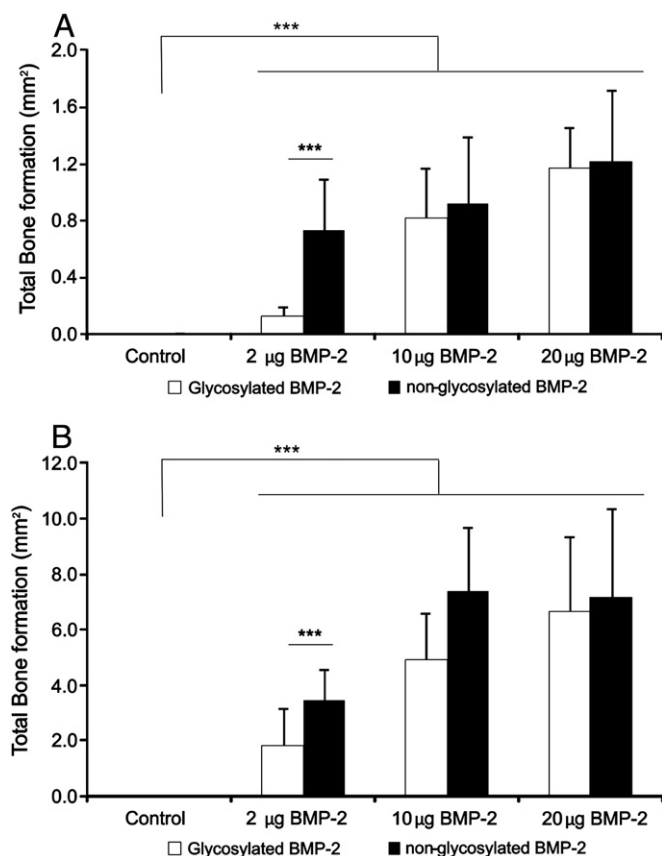


Fig. 7. Osteoinductive capacity of gBMP-2 and ngBMP-2 loaded carriers at an ectopic location after 4 (A) and 12 (B) weeks implantation period. Bone formation is only observed in the BMP-2 loaded carriers. In addition, ngBMP-2 can significantly induce more bone at lower concentrations compared to gBMP-2 at both implantation periods. Error bars represent means \pm standard deviation. (***) = $p < 0.001$; $n > 7$.

the implants are suggested to be responsible for this observation. This higher retention of ngBMP-2 corroborates earlier findings [25] that indicated a decreased solubility of ngBMP-2 in fibrin matrices. Additionally, this indicates that the biological activity of BMP-2 is not directly depending on release but rather on availability and solubility, in either released or bound form, in a specific area.

The sustained release and thus bone formation is carrier dependent due to altered release rates of BMP-2 from the different carriers [12]. For example, the retention of gBMP-2 within an alginate mesh is significantly increased compared to a collagen sponge in the first week after which the difference diminishes [38]. Together with the finding of Brown et al., who reported a positive effect on bone formation after a BMP-2 burst release and a subsequent sustained release, it was suggested that a combination of relatively high initial release and a low sustained release thereafter may be beneficial for growth factor efficacy [39]. The release kinetics observed in the current study corroborate earlier findings and indicate a similar effect [37]. However, the BMP-2 activation in relation to the bioactivity of BMP-2 needs to be observed as a complex factor. It is assumed that BMP-2 not only acts in released form, but also when it is presented in an adsorbed form to the target cells [20,40]. However, up to date the ability to discriminate the contribution of adsorbed and released forms of BMP-2 is not available.

The induction of ectopic bone tissue by BMP-2 adsorbed to pre-set CPC scaffolds showed to be both dose- and time-dependent with significantly higher bone formation induced by ngBMP-2 at low dosage compared to gBMP-2. The amount of ectopic bone formation was comparable to previous experiments with subcutaneous implantation of scaffolds containing adsorbed glycosylated (rh)BMP-2 [18,41].

Bone tissue was predominantly formed in the periphery of the porous CPC scaffolds as well as at the material/tissue interface. This observation is likely related to the rapid and strong interaction between proteins (e.g. BMP-2) and the pre-set CPC scaffolds and the limitations micrometer-scale porosity brings along regarding cell penetration. In general, proteins rapidly adsorb to CaP-based materials due to electrostatic interactions [42], which even can become stronger upon conformational changes of adsorbed proteins. More particularly, Ruhé et al. studied the effect of albumin pre-treatment of pre-set, porous CPC scaffolds on BMP-2 release under different conditions [43] and demonstrated that albumin pre-treatment only had a marginal effect on the limited release of BMP-2, emphasizing the capacity of pre-set CPC scaffolds to retain adsorbed proteins. Penetration of (bone) tissue into a porous relies on the size of the pores and their interconnectivity. In relation to CPC, Link et al. demonstrated that tissue ingrowth into pre-set CPC scaffolds containing PLGA-microparticles occurred when pore size exceeded 50 μm and interconnectivity was obtained by incorporating sufficient porogen, in their case at least 20 wt.% PLGA-microparticles [44]. The pre-set porous CPC scaffolds used in the present study were made using smaller PLGA-microparticles (i.e. 40 μm) and a higher amount (i.e. 30 wt.%). Based on the observations that bone formation and tissue ingrowth were limited to the periphery of the pre-set CPC scaffolds, as additionally shown using paraffin-embedded decalcified sections, the created porosity within these scaffolds apparently was insufficient for cell penetration.

In summary, the present study revealed that ngBMP-2 is less biologically active in vitro compared to gBMP-2, however still capable of inducing osteoblast-like cells to differentiate and mineralize. In addition, ngBMP-2 showed slower release from a CaP-based implant compared to gBMP-2. Despite lower biological activity and release in vitro, ngBMP-2 significantly increased ectopic bone formation at low dosages. This observation provides strong evidence that the efficacy of ngBMP-2 in vivo is enhanced compared to gBMP-2 and reflects its value for enrichment strategies for biomaterials, bone tissue engineering and bone regenerative treatments.

Acknowledgments

The authors gratefully acknowledge the support of the Smart Mix Program of the Netherlands Ministry of Economic Affairs and The Netherlands Ministry of Education, Culture and Science. The authors would like to thank Natasja van Dijk for assistance with the histological preparations, Cathelijne Frielink for help with ^{125}I -BMP-2 release experiments and Dr. Ir. Ewald Bronkhorst for assistance with statistical analyses. Scanning electron microscopy was performed at the Nijmegen Center for Molecular Life Sciences (NCMLS), the Netherlands.

References

- [1] P.D. Delmas, M. Anderson, Launch of the bone and joint decade 2000–2010, *Osteoporos. Int.* 11 (2000) 95–97.
- [2] L.C. Chow, Next generation calcium phosphate-based biomaterials, *Dent. Mater. J.* 28 (2009) 1–10.
- [3] M.P. Ginebra, M. Espanol, E.B. Montufar, R.A. Perez, G. Mestres, New processing approaches in calcium phosphate cements and their applications in regenerative medicine, *Acta Biomater.* 6 (2010) 2863–2873.
- [4] M.N. Rahaman, D.E. Day, B. Sonny Bal, Q. Fu, S.B. Jung, L.F. Bonewald, A.P. Tomsia, Bioactive glass in tissue engineering, *Acta Biomater.* 7 (2011) 2355–2373.
- [5] P.A. Gunatillake, R. Adhikari, Biodegradable synthetic polymers for tissue engineering, *Eur. Cell Mater.* 5 (2003) 1–16.
- [6] C. Xu, P. Su, X. Chen, Y. Meng, W. Yu, A.P. Xiang, Y. Wang, Biocompatibility and osteogenesis of biomimetic bioglass-collagen-phosphatidylserine composite scaffolds for bone tissue engineering, *Biomaterials* 32 (2011) 1051–1058.
- [7] P. Ruhé, E. Hedberg-Dirk, N.T. Padron, P. Spauwen, J. Jansen, A. Mikos, Porous poly(DL-lactic-co-glycolic acid)/calcium phosphate cement composite for reconstruction of bone defects, *Tissue Eng.* 12 (2006) 789–800.
- [8] P.C. Bessa, M. Casal, R.L. Reis, Bone morphogenetic proteins in tissue engineering: the road from the laboratory to the clinic, part I (basic concepts), *J. Tissue Eng. Regen. Med.* 2 (2008) 1–13.

- [9] P.C. Bessa, M. Casal, R.L. Reis, Bone morphogenetic proteins in tissue engineering: the road from laboratory to clinic, part II (BMP delivery), *J. Tissue Eng. Regen. Med.* 2 (2008) 81–96.
- [10] J.A. Jansen, J.W.M. Vehof, P.Q. Ruhé, H. Kroese-Deutman, Y. Kuboki, H. Takita, E.L. Hedberg, A.G. Mikos, Growth factor-loaded scaffolds for bone engineering, *J. Control. Release* 101 (2005) 127–136.
- [11] X. Cao, D. Chen, The BMP signaling and in vivo bone formation, *Gene* 357 (2005) 1–8.
- [12] H. Seeherman, J.M. Wozney, Delivery of bone morphogenetic proteins for orthopedic tissue regeneration, *Cytokine Growth Factor Rev.* 16 (2005) 329–345.
- [13] R.D. Welch, A.L. Jones, R.W. Bucholz, C.M. Reinert, J.S. Tjia, W.A. Pierce, J.M. Wozney, X.J. Li, Effect of recombinant human bone morphogenetic protein-2 on fracture healing in a goat tibial fracture model, *J. Bone Miner. Res.* 13 (1998) 1483–1490.
- [14] K. Bessho, D.L. Carnes, R. Cavin, J.L. Ong, Experimental studies on bone induction using low-molecular-weight poly(DL-lactide-co-glycolide) as a carrier for recombinant human bone morphogenetic protein-2, *J. Biomed. Mater. Res.* 61 (2002) 61–65.
- [15] M. Isobe, Y. Yamazaki, M. Mori, K. Ishihara, N. Nakabayashi, T. Amagasa, The role of recombinant human bone morphogenetic protein-2 in PLGA capsules at an extraskeletal site of the rat, *J. Biomed. Mater. Res.* 45 (1999) 36–41.
- [16] L. Luca, A.-L. Rougemont, B.H. Walpoth, L. Boure, A. Tami, J.M. Anderson, O. Jordan, R. Gurny, Injectable rhBMP-2-loaded chitosan hydrogel composite: osteoinduction at ectopic site and in segmental long bone defect, *J. Biomed. Mater. Res. A* 96A (2011) 66–74.
- [17] P.Q. Ruhé, H.C. Kroese-Deutman, J.G.C. Wolke, P.H.M. Spauwen, J.A. Jansen, Bone inductive properties of rhBMP-2 loaded porous calcium phosphate cement implants in cranial defects in rabbits, *Biomaterials* 25 (2004) 2123–2132.
- [18] H.C. Kroese-Deutman, P.Q. Ruhé, P.H.M. Spauwen, J.A. Jansen, Bone inductive properties of rhBMP-2 loaded porous calcium phosphate cement implants inserted at an ectopic site in rabbits, *Biomaterials* 26 (2005) 1131–1138.
- [19] L. Zhao, M. Tang, M.D. Weir, M.S. Detamore, H.H.K. Xu, Osteogenic media and rhBMP-2-induced differentiation of umbilical cord mesenchymal stem cells encapsulated in alginate microbeads and integrated in an injectable calcium phosphate-chitosan fibrous scaffold, *Tissue Eng. Part A* 17 (2011) 969–979.
- [20] E. Bodde, O. Boerman, F. Russel, A. Mikos, P. Spauwen, J. Jansen, The kinetic and biological activity of different loaded rhBMP-2 calcium phosphate cement implants in rats, *J. Biomed. Mater. Res. A* 87A (2008) 780–791.
- [21] J.W.M. Vehof, A.E. de Ruijter, P.H.M. Spauwen, J.A. Jansen, Influence of rhBMP-2 on rat bone marrow stromal cells cultured on titanium fiber mesh, *Tissue Eng.* 7 (2001) 373–383.
- [22] J. van den Dolder, A.J.E. de Ruijter, P.H.M. Spauwen, J.A. Jansen, Observations on the effect of BMP-2 on rat bone marrow cells cultured on titanium substrates of different roughness, *Biomaterials* 24 (2003) 1853–1860.
- [23] R.E. Jung, F.E. Weber, D.S. Thoma, M. Ehrbar, D.L. Cochran, C.H.F. Hammerle, Bone morphogenetic protein-2 enhances bone formation when delivered by a synthetic matrix containing hydroxyapatite/tricalciumphosphate, *Clin. Oral Implants Res.* 19 (2008) 188–195.
- [24] T.K. Sampath, J.E. Coughlin, R.M. Whetstone, D. Banach, C. Corbett, R.J. Ridge, E. Ozkaynak, H. Oppermann, D.C. Rueger, Bovine osteogenic protein is composed of dimers of OP-1 and BMP-2A, two members of the transforming growth factor-beta superfamily, *J. Biol. Chem.* 265 (1990) 13198–13205.
- [25] H. Schmoekel, J.C. Schense, F.E. Weber, K.W. Grätz, D. Gnägi, R. Müller, J.A. Hubbell, Bone healing in the rat and dog with nonglycosylated BMP-2 demonstrating low solubility in fibrin matrices, *J. Orthop. Res.* 22 (2004) 376–381.
- [26] K. Sariirahimoglu, S.C.G. Leeuwenburgh, J.G.C. Wolke, L. Yubao, J.A. Jansen, Effect of calcium carbonate on hardening, physicochemical properties, and in vitro degradation of injectable calcium phosphate cements, *J. Biomed. Mater. Res. A* 100A (3) (2012) 712–719.
- [27] T. Katagiri, A. Yamaguchi, T. Ikeda, S. Yoshiki, J.M. Wozney, V. Rosen, E.A. Wang, H. Tanaka, S. Omura, T. Suda, The non-osteogenic mouse pluripotent cell line, C3H10T1/2, is induced to differentiate into osteoblastic cells by recombinant human bone morphogenetic protein-2, *Biochem. Biophys. Res. Commun.* 172 (1990) 295–299.
- [28] E. Piek, L.S. Sleumer, E.P. van Someren, L. Heuver, J.R. de Haan, I. de Grijns, C. Gilissen, J.M. Hendriks, R.I. van Ravestein-van Os, S. Bauerschmidt, K.J. Decherling, E.J. van Zoelen, Osteo-transcriptomics of human mesenchymal stem cells: accelerated gene expression and osteoblast differentiation induced by vitamin D reveals c-MYC as an enhancer of BMP2-induced osteogenesis, *Bone* 46 (2010) 613–627.
- [29] C.W.G.M. Lowik, M.J. Alblas, M. Vanderluit, S.E. Papapoulos, G. Vanderpluijm, Quantification of adherent and nonadherent cells cultured in 96-well plates using the supravital stain neutral red, *Anal. Biochem.* 213 (1993) 426–433.
- [30] C. Maniopoulos, J. Sodek, A.H. Melcher, Bone formation in vitro by stromal cells obtained from bone marrow of young adult rats, *Cell Tissue Res.* 254 (1988) 317–330.
- [31] W. Habraken, J. Wolke, A. Mikos, J. Jansen, Injectable PLGA microsphere/calcium phosphate cements: physical properties and degradation characteristics, *J. Biomater. Sci. Polym. Ed.* 17 (2006) 1057–1074.
- [32] H. van der Lubbe, C. Klein, K. de Groot, A simple method for preparing thin (10 microm) histological sections of undecalcified plastic embedded bone with implants, *Stain. Technol.* 63 (1988) 171–176.
- [33] P.J. Fraker, J.C. Speck, Protein and cell membrane iodinations with a sparingly soluble chloroamide, 1,3,4,6-tetrachloro-3a,6a-diphenylglycoluril, *Biochem. Biophys. Res. Commun.* 80 (1978) 849–857.
- [34] S. Zerbs, A.M. Frank, F.R. Collart, Bacterial systems for production of heterologous proteins, *Methods Enzymol.* 463 (2009) 149–168.
- [35] S. Long, L. Truong, K. Bennett, A. Phillips, F. Wong-Staal, H. Ma, Expression, purification, and renaturation of bone morphogenetic protein-2 from *Escherichia coli*, *Protein Expr. Purif.* 46 (2006) 374–378.
- [36] K. Yano, M. Hoshino, Y. Ohta, T. Manaka, Y. Naka, Y. Imai, W. Sebald, K. Takaoka, Osteoinductive capacity and heat stability of recombinant human bone morphogenetic protein-2 produced by *Escherichia coli* and dimerized by biochemical processing, *J. Bone Miner. Metab.* 27 (2009) 355–363.
- [37] W.J.E.M. Habraken, O.C. Boerman, J.G.C. Wolke, A.G. Mikos, J.A. Jansen, *In vitro* growth factor release from injectable calcium phosphate cements containing gelatin microspheres, *J. Biomed. Mater. Res. A* 91A (2009) 614–622.
- [38] J.D. Boerckel, Y.M. Kolambkar, K.M. Dupont, B.A. Uhrig, E.A. Phelps, H.Y. Stevens, A.J. Garcia, R.E. Guldberg, Effects of protein dose and delivery system on BMP-mediated bone regeneration, *Biomaterials* 32 (2011) 5241–5251.
- [39] K.V. Brown, B. Li, T. Guda, D.S. Perrien, S.A. Guelcher, J.C. Wenke, Improving bone formation in a rat femur segmental defect by controlling bone morphogenetic protein-2 release, *Tissue Eng. Part A* 17 (2011) 1735–1746.
- [40] H. Uludag, D. D'Augusta, J. Golden, J. Li, G. Timony, R. Riedel, J. Wozney, Implantation of recombinant human bone morphogenetic proteins with biomaterial carriers: a correlation between protein pharmacokinetics and osteoinduction in the rat ectopic model, *J. Biomed. Mater. Res. A* 50 (2000) 227–238.
- [41] J. Lee, C. Kim, K. Choi, U. Jung, J. Yun, S. Choi, K. Cho, The induction of bone formation in rat calvarial defects and subcutaneous tissues by recombinant human BMP-2, produced in *Escherichia coli*, *Biomaterials* 31 (2010) 3512–3519.
- [42] T.S. Tsapikouni, Y.F. Missirlis, Protein-material interactions: from micro-to-nano scale, *Mater. Sci. Eng. B* 152 (2008) 2–7.
- [43] P. Ruhé, O. Boerman, F. Russel, A. Mikos, P. Spauwen, J. Jansen, *In vivo* release of rhBMP-2 loaded porous calcium phosphate cement pretreated with albumin, *J. Mater. Sci. Mater. Med.* 17 (2006) 919–927.
- [44] D.P. Link, J. van den Dolder, J.J.P. van den Beucken, V.M. Cuijpers, J.G.C. Wolke, A.G. Mikos, J.A. Jansen, Evaluation of the biocompatibility of calcium phosphate cement/PLGA microparticle composites, *J. Biomed. Mater. Res. A* 87A (2008) 760–769.